

NoiLIn: Do Noisy Labels Always Hurt Adversarial Training?

Jingfeng Zhang^{*1}, Xilie Xu^{*2,3}, Bo Han^{4,1}, Tongliang Liu⁵,
Gang Niu¹, Lizhen Cui⁶, and Masashi Sugiyama^{1,7}

¹RIKEN Center for Advanced Intelligence Project (AIP), Tokyo, Japan

²Taishan College, Shandong University, Jinan, China

³School of Computing, National University of Singapore, Singapore

⁴Department of Computer Science, Hong Kong Baptist University, Hong Kong SAR, China

⁵Trustworthy Machine Learning Lab, University of Sydney, Sydney, Australia

⁶School of Software & Joint SDU-NTU Centre for Artificial Intelligence Research
(C-FAIR), Shandong University, Jinan, China

⁷Graduate School of Frontier Sciences, University of Tokyo, Tokyo, Japan

Abstract

Adversarial training (AT) based on *minimax* optimization is a popular learning style that enhances the model’s *adversarial robustness*. Noisy labels (NL) commonly undermine the learning and hurt the model’s performance. Interestingly, both research directions have hardly crossed and hit sparks. In this paper, we raise an intriguing question—Does NL always hurt AT? Firstly, we find that NL injection in *inner maximization for generating adversarial data* augments natural data implicitly, which benefits AT’s generalization. Secondly, we find NL injection in *outer minimization for the learning* serves as regularization that alleviates robust overfitting, which benefits AT’s robustness. To enhance AT’s adversarial robustness, we propose “NoiLIn” that gradually increases Noisy Labels Injection over the AT’s training process. Empirically, NoiLIn answers the previous question negatively—the adversarial robustness can be indeed enhanced by NL injection. Philosophically, we provide a new perspective of the learning with NL: NL should not always be deemed detrimental, and even in the absence of NL in the training set, we may consider injecting it deliberately.

1 Introduction

Security-related areas require deep models to be adversarially robust against *adversarial attack* [30]. To obtain *adversarial robustness*, *adversarial training* (AT) [20] would be currently the most effective defense that has so far not been comprehensively compromised [4]. AT is formulated as a minimax optimization problem with the *inner maximization* to generate adversarial data and the *outer minimization* to learn from the generated adversarial data [20].

To enhance adversarial robustness further, AT methods have mainly focused on manipulating the inner maximization or the outer minimization [5, 34, 29, 41, 6, 32, 43, 38, 44, 42, 33, 35]. For example, by manipulating the inner maximization for generating quality adversarial data, Wang et al. [32] gradually increased the convergence quality of the generated adversarial data; Zhang et al. [43] generated *friendly adversarial data* that are near the decision boundaries but are wrongly classified. On the other hand, by manipulating the outer minimization for designing the model’s loss functions for the learning, Zhang et al. [42] designed TRADES that has two loss terms, i.e., the cross entropy loss on the natural data and the Kullback-Leibler (KL) divergence loss on the adversarial data. Meanwhile, Wang et al. [33] designed MART that is composed of the boosted cross entropy loss and the guided KL divergence loss, both on the adversarial data.

^{*}Equal Contributions.

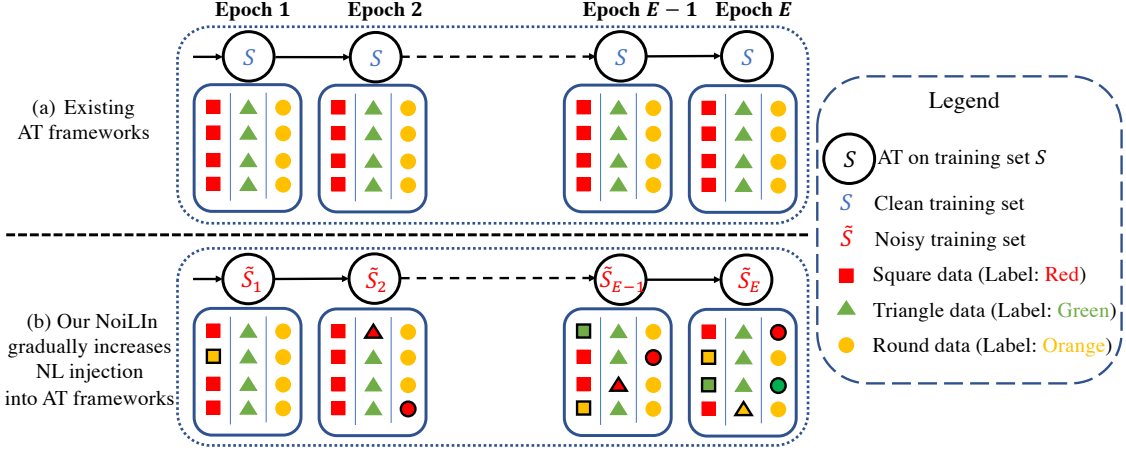


Figure 1: Comparisons between the existing AT framework (panel (a)) and our AT-NoiLIn framework (panel (b)). At each training epoch, AT-NoiLIn randomly flips labels of a portion of data (marked in the black edges), generating noisy-label training set \tilde{S} for the learning.

Despite active investigations of either generating quality adversarial data or designing loss functions for optimizing those data, little effort has been made to investigate noisy labels (NL) in AT since *NL is often deemed to hurt the training*. Essentially, noisy labels are flipped from ground-truth labels [2], and thus they are often deemed to hurt the learned models in standard training (ST) [40]. For example, deep models in ST can easily memorize NL that leads to the degradation of generalization [3]; NL causes significant adversarial vulnerability of learned models in ST [28]. To combat NL, there are many proposals, such as sample selection [18, 16] and loss/label correction [26, 24, 15, 36]. Therefore, it seems a counter-intuitive suggestion to benefit AT by leveraging NL.

However, in this paper, we investigate two cases where *injecting NL benefits AT*. First, we inject NL in inner maximization (see Section 3). In each training minibatch, we randomly choose a portion of data whose adversarial variants are generated according to the flipped labels; the labels in outer minimization are intact for the learning. The flipped-label adversarial variants are far from the decision boundaries, which does not help to enhance adversarial robustness [13, 44]; instead, they augment the natural data, which benefits the generalization. Therefore, injecting NL in inner maximization does not enhance robustness but improves generalization of AT.

Second, we inject NL in outer minimization (see Section 4). We generate the adversarial data in each training minibatch according to the intact labels but randomly flip a portion of labels for the learning. Injecting NL in outer minimization leads to a high data variance for the learning, thus, making the model difficult to fit the adversarial data. Therefore, it serves as regularization to largely alleviate robust overfitting [27] and enhance AT’s adversarial robustness.

Inspired by the above two cases, we propose our method “*NoiLIn*” that automatically adjusts NL injection into AT (see Figure 1 and Section 5.1). In each training epoch, we first randomly flip a portion of labels of the training set, and then execute an AT method using the noisy-label set. As the training progresses, we increase the flipping portion if there occurs robustness degradation (evaluated on a validation set). Our simple yet effective strategy is easily compatible with various AT methods, which does not hurt or even boost their adversarial robustness consistently over training epochs.

Our contributions are as follows. (a) We conduct a study of NL from a novel perspective: injecting NL in inner maximization can benefit AT’s generalization; injecting NL in outer minimization can benefit AT’s robustness. (b) We propose a general method, i.e., NoiLIn, which can be easily incorporated into existing AT methods. Empirically, our NoiLIn can relieve the issue of robust overfitting [27] and even lead to improved robustness with negligible degradation of generalization. (c) Philosophically, we should not always consider NL to be detrimental. Even in the absence of NL in the training set, we may consider injecting it deliberately.

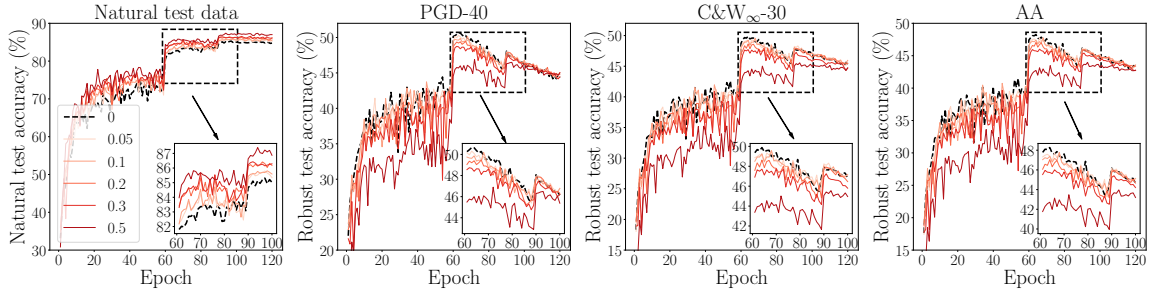


Figure 2: The learning curves of injecting various levels of symmetric-flipping NL in inner maximization. The number in the legend represents noise rate η . Pair-flipping NL injection is in Appendix B.

2 Background and Related Work

This section briefly reviews the background of AT and provides related works on the interaction between AT and NL.

2.1 Adversarial Training (AT)

We review the learning objective of AT [20] as follows.

Let (\mathcal{X}, d_∞) be the input feature space \mathcal{X} with the infinity distance metric $d_{\text{inf}}(x, x') = \|x - x'\|_\infty$, and

$$\mathcal{B}_\epsilon[x] = \{x' \in \mathcal{X} \mid d_{\text{inf}}(x, x') \leq \epsilon\}$$

be the closed ball of radius $\epsilon > 0$ centered at x in \mathcal{X} . Given a dataset $S = \{(x_i, y_i)\}_{i=1}^n$, where $x_i \in \mathcal{X}$ and $y_i \in \mathcal{Y} = \{0, 1, \dots, C-1\}$, the learning objective function is formulated as a minimax optimization problem, i.e.,

$$\underbrace{\min_{f \in \mathcal{F}} \frac{1}{n} \sum_{i=1}^n \ell(f(\tilde{x}_i), y_i)}_{\text{outer minimization}}, \quad \underbrace{\tilde{x}_i = \arg \max_{\tilde{x} \in \mathcal{B}_\epsilon[x_i]} \ell(f(\tilde{x}), y_i)}_{\text{inner maximization}}. \quad (1)$$

Eq. (1) implies the AT’s realization with one step of *inner maximization* to generate adversarial data \tilde{x}_i and one step of *outer minimization* on learning the generated adversarial data.

Many existing defense methods [20, 42, 33, 43, 44, 8, 1, 21] and adversarial attacks [14, 7, 11, 4] implicitly assume labels y_i are intact in Eq. (1). In this paper, we deliberately inject NL and explore the effects of flipped label \tilde{y}_i in AT.

2.2 Interaction between NL and AT

Noisy labels (NL) practically exist in the training set [22], and some studies have explored the interaction between NL and AT. Alayrac et al. [1] showed that NL degraded both generalization and robustness of AT, but generalization suffers less from NL than robustness. Sanyal et al. [28] showed robust training avoids memorization of NL, and Zhu et al. [45] showed AT has smoothing effect which can naturally mitigate the negative effect of NL. Nevertheless, all those studies deemed NL detrimental and considered eliminating NL during the training.

In this paper, we assume the training set is noise-free, and we treat NL as a friend and deliberately inject NL for benefiting adversarial robustness. This paper mainly focuses on injecting two typical class-conditional NL: 1) *symmetric-flipping noise* [31], where labels y_i are flipped at random with the uniform distribution; 2) *pair-flipping noise* [16], where labels y_i are flipped between adjacent classes that are prone to be mislabeled.

3 NL Injection in Inner Maximization

In this section, we investigate NL injection in AT’s inner maximization. In Section 3.1, we empirically show that injecting NL in inner maximization does not improve robustness but enhances generalization. In Section 3.2, we explore the reasons for those phenomena.

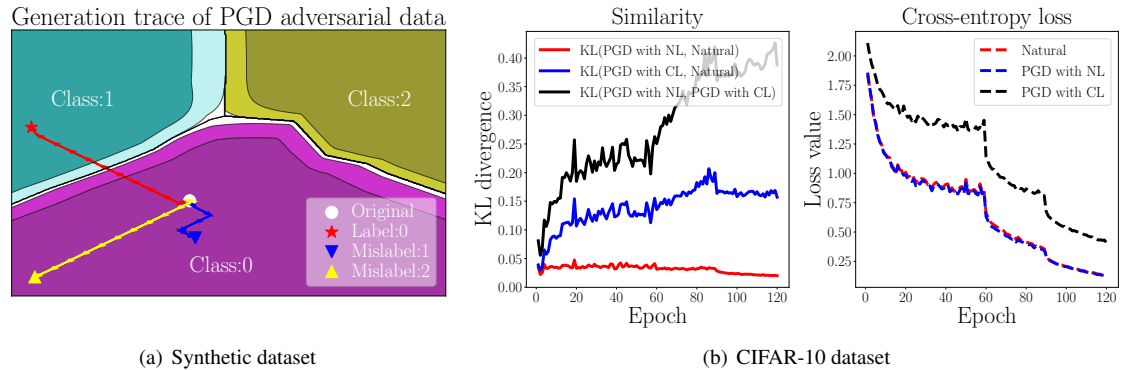


Figure 3: Figure 3(a) shows the adversarial data generation traces on a synthetic ternary classification dataset. The red trace was generated with CL; both yellow and blue traces were generated with NL. The color gradient represents the prediction confidence: the deeper color represents higher prediction confidence. Figure 3(b) shows the similarity among PGD with CL, PGD with symmetric-flipping NL ($\eta = 1$), and natural data as well as their corresponding inner loss on CIFAR-10.

3.1 NL Injection in Inner Maximization Improves Generalization

We conducted empirical experiments of injecting NL in inner maximization on CIFAR-10 dataset [19]. In Figure 2, we compared AT with NL in inner maximization (red lines with different shades) and standard AT (black dashed lines). We injected symmetric-flipping NL into inner maximization. In each training mini-batch, we randomly flipped η portion of labels of training data. The adversarial data were generated according to the flipped labels. The noise rate η was sampled from $\{0, 0.05, 0.1, 0.2, 0.3, 0.5\}$. Note that it is exactly standard AT when $\eta = 0$. The perturbation bound was set to $\epsilon_{\text{train}} = 8/255$; the number of projected gradient descent (PGD) steps was set to $K = 10$ and the step size was set to $\alpha = 2/255$. The labels of outer minimization were intact for the learning. We trained ResNet-18 [17] using SGD with 0.9 momentum for 120 epochs with the initial learning rate of 0.1 divided by 10 at Epochs 60 and 90, respectively.

We evaluated the robust models based on the four evaluation metrics, i.e., standard test accuracy on natural test data, robust test accuracy on adversarial data generated by PGD-40 [8], C&W $_{\infty}$ -30 (L_{∞} version of C&W [7] optimized by PGD-30), and AutoAttack [11] (AA), respectively. The adversarial test data were bounded by L_{∞} perturbations with $\epsilon_{\text{test}} = 8/255$. We demonstrated the learning curves of injecting symmetric-flipping NL in Figure 2 and deferred those of pair-flipping NL in Appendix B.

In terms of generalization, robust models trained by injecting NL in inner maximization (red lines with different shades) obtained higher standard test accuracy compared with those trained by standard AT (black dashed lines). Standard test accuracy increased as noise rate η increased. In terms of robustness, with the increasing of η , robust test accuracy only dropped slightly at the best checkpoint (at around Epoch 60). At the final epochs (e.g., at Epochs 90 – 120), the robustness was comparable with standard AT, especially for $\eta \leq 0.3$. Empirically, injecting NL in inner maximization was shown to be beneficial to AT’s generalization with slight degradation of robustness.

3.2 NL Injection in Inner Maximization Implicitly Augments Natural Data

Here, we explore why injecting NL in inner maximization improves generalization. We analyze the effects of NL on generating adversarial data: NL impedes the optimizer to find correct directions to the decision boundary; as a result, the generated PGD adversarial data with NL are similar to their natural data. Therefore, injecting NL in inner maximization implicitly augments natural data, thus benefiting generalization.

In Figure 3(a), we drew the generation traces of PGD adversarial data on a two-dimensional ternary classification dataset. We randomly chose a start point (white dot) whose correct label (CL) is 0 and plotted the generation traces of adversarial data using correct label 0 (red trace), wrong label 1 (blue trace), and wrong label 2 (yellow trace), respectively. We found that NL (wrong label 1 or 2) misled the generation traces that should have pointed at the decision boundary. Instead, generation traces with NL fell in the internal areas of class 0. Therefore, the generated adversarial data with NL were similar to class 0’s natural data.

To further justify the above phenomenon, in Figure 3(b), we used a real-world dataset—CIFAR-10—to reveal the similarity among “PGD with NL” (PGD adversarial data with wrong labels), “PGD with CL”

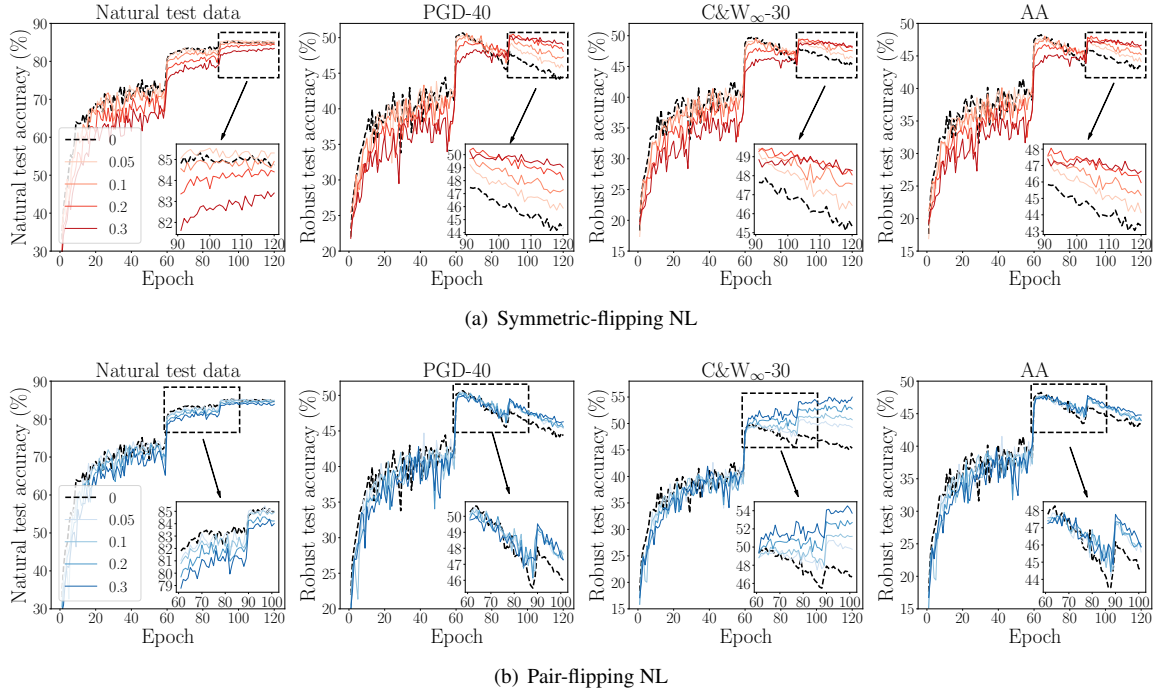


Figure 4: The learning curves of injecting various levels of NL in outer minimization. The number in the legend represents noise rate η .

(PGD adversarial data with correct labels), and “Natural” (natural data). We conducted a standard adversarial training for 120 epochs and saved the model’s checkpoint at every epoch. At every checkpoint, we randomly selected 1000 training data and generated “PGD with NL” and “PGD with CL” of these data. We used model’s Kullback–Leibler (KL) loss [42] as the similarity metric (the smaller value means larger similarity). In the left panel of Figure 3(b), we compared similarity among “PGD with NL”, “PGD with CL”, and “Natural”. In addition, in the right panel of Figure 3(b), we used the correct labels to calculate the cross-entropy loss of “PGD with NL”, “PGD with CL”, and “Natural”, respectively.

The left panel of Figure 3(b) shows that the value of $\text{KL}(\text{PGD with NL}, \text{Natural})$ (red solid line) is apparently lower than that of $\text{KL}(\text{PGD with CL}, \text{Natural})$ (blue solid line). Besides, the right panel of Figure 3(b) shows that the cross-entropy loss of “PGD with NL” is almost identical to that of “Natural”. Compared with “PGD with CL”, “PGD with NL” is more similar to “Natural” (natural data). Therefore, NL injection in inner maximization implicitly augments natural data, which benefits natural generalization.

4 NL Injection in Outer Minimization

In Section 4.1, we observe that NL injection in outer minimization can mitigate the undesirable issue of robust overfitting; besides, it can largely improve model’s robustness against some specific types of attack, e.g., C&W attack. In Section 4.2, we provide the explanations for these intriguing phenomena.

4.1 Injecting NL in Outer Minimization Alleviates Robust Overfitting

To explore NL in outer minimization, in Figures 4(a) and 4(b), we showed the results of a series of experiments with various NL levels η injected in outer minimization. We adversarially trained ResNet-18 on the CIFAR-10 dataset. Adversarial data were generated according to the intact labels. We randomly chose an η portion of adversarial data at each training minibatch to flip their labels for the learning. The detailed training settings (e.g., the learning rate schedule and optimizer) kept the same as Section 3.1. We showed the learning curves of injecting symmetric-flipping NL (in Figure 4(a)) and pair-flipping NL (in Figure 4(b)). We compared the learned models (red and blue lines with different shades) with those by standard AT (black dashed lines) at every training epoch. We reported generalization performance by evaluating models on natural test data and reported robustness performance by evaluating models on adversarial test data that were generated by PGD-40, C&W $_{\infty}$ -30, and AA attacks, respectively. Note that we did not show $\eta > 0.3$ since injecting too much noise in outer minimization destabilized or even baffled the training.

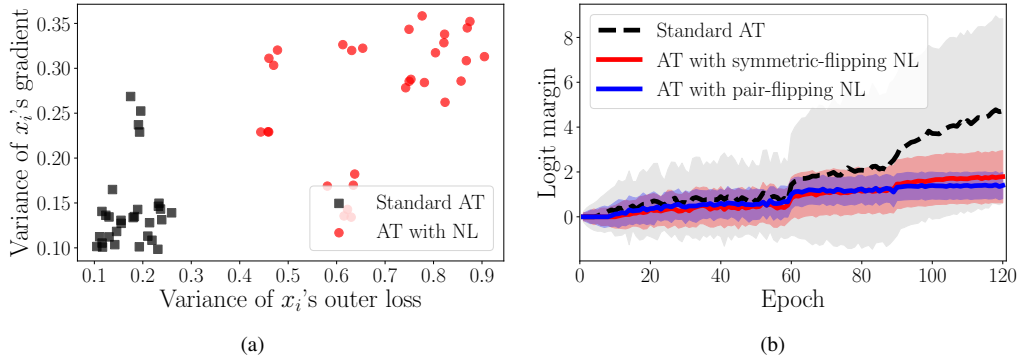


Figure 5: Figure 5(a) compares the *variance* of *data’s outer loss* (vertical axis) and *data’s gradient* (horizontal axis) over the training process of standard AT (black squares) with that of AT with symmetric-flipping NL in outer minimization (red rounds). Figure 5(a) shows that NL in outer minimization leads to high data variance, thus impeding overfitting. Figure 5(b) compares the median *logit margin* of natural test data and its standard deviation over the training process of standard AT (black dashed line), that of AT with symmetric-flipping NL in outer minimization (red line), and that of AT with pair-flipping NL in outer minimization (blue line). Figure 5(b) shows that NL in outer minimization reduces logit margins, thus obfuscating gradients of the C&W attack [7].

In Figure 4, we observed that injecting NL leads to consistently better robustness than AT (black dashed line) at several last epochs. Besides, as the noise rate η increases (the color gradually becomes deeper) the robustness at the final epoch improves as well. This implies that injecting more NL in outer minimization can alleviate robust overfitting to a larger degree. In addition, we found an intriguing phenomenon that in the third panel of Figure 4(b), injecting pair-flipping NL can largely improve the model’s robustness against the C&W $_{\infty}$ -30 attack. We defer the detailed explanations to Section 4.2.

Therefore, based on our empirical observations, NL should not always be considered to be detrimental. Even in the absence of NL in the training dataset, we may deliberately inject some NL in outer minimization to benefit the adversarial robustness.

4.2 Why Does NL in Outer Minimization Help?

Next, we investigate why injecting NL in outer minimization alleviates the robust overfitting and benefits adversarial robustness against the C&W attack.

NL in outer minimization induces high data variance and thereby impedes overfitting. Robust overfitting [27] is an undesirable phenomenon in AT, where after the first learning rate decay, the model’s robustness stops increasing but begins to decrease. To remedy the robust overfitting, recent studies have proposed early stopping the training [27], injecting the learned smoothing [9], and focusing on near-decision-boundary data [44]. In essence, those efforts tried to maintain the data’s high variance during the training, thus impeding overfitting.

Simply injecting NL in outer minimization can also incur high data variance. In Figure 5(a), we compared the data’s variance between the training process of standard AT (black squares) and that of AT with NL (red rounds). We randomly appointed 30 training data for standard AT and AT with NL and collected the training statistics of each data point over 120 training epochs. For each data point x_i , we can collect a 120-dimensional vector. Firstly, we collected a 120-dimensional vector of x_i ’s *outer loss* (horizontal axis)—the loss of the generated adversarial data, i.e., $\ell(f(\tilde{x}_i), \tilde{y}_i)$. Secondly, we collected a 120-dimensional vector of x_i ’s *gradients* (vertical axis)—the ℓ_2 norm of the weight gradient on $(\tilde{x}_i, \tilde{y}_i)$, i.e., $\|\nabla_{\theta} \ell(f(\tilde{x}_i), \tilde{y}_i)\|_2$. Then, we calculated the variance over x_i ’s 120-dimensional vectors. Therefore, we had 30 red points for AT with NL and 30 black points for standard AT. Note that over the training process, \tilde{y}_i was always equal to y_i for standard AT but not always equal to y_i for AT with NL.

Figure 5(a) shows that red rounds are clustered at the upper right, and black squares are clustered at the lower left, which justifies that AT with NL has higher data variance than standard AT. Therefore, injecting

Algorithm 1 NoiLIn: Boost AT via automatically increasing Noisy Labels Injection

Input: network f_θ , training set S_{train} , validation set S_{valid} , total epochs E , initial noise rate η_{min} , maximal noise rate η_{max} , sliding window size τ , boosting rate γ

Output: adversarially robust network f_θ

$\eta = \eta_{\text{min}}$

for Epoch $e = 1, \dots, E$ **do**

 Randomly flip η portion of labels of training dataset S_{train} to get \tilde{S}

 Update f_θ using \tilde{S} by an AT method

 Obtain robust validation accuracy \mathcal{A}_e using S_{valid}

if $\sum_{i=e-\tau}^e \mathcal{A}_i < \sum_{j=e-\tau-1}^{e-1} \mathcal{A}_j$ **then**

$\eta = \min(\eta \cdot (1 + \gamma), \eta_{\text{max}})$

 // Boost NL injection rate η if robust overfitting occurs.

end if

end for

NL in outer minimization can induce high data variance, thereby impeding the undesirable issue of robust overfitting.

NL in outer minimization obfuscates gradients of the C&W attack. From Figure 3, we observed that NL in outer minimization can significantly improve the model’s robustness against the C&W attack, especially injecting pair-flipping label noise.

To figure out the reason for this phenomenon, at every training epoch, we illustrated the median *logit margin* $f_\theta^y(x) - \max_{j \neq y} f_\theta^j(x)$ over all natural test data and its standard deviation in Figure 5(b). We compared standard AT (black dashed line) with AT with NL (the red line for injecting symmetric noise and the blue line for injecting pair flipping noise). As shown in Figure 5(b), injecting NL in outer minimization leads to a small logit margin, especially injecting pair-flipping NL (the blue line). Note that the implementation of the C&W attack follows

$$\tilde{x} = \arg \max_{\tilde{x} \in \mathcal{B}_\epsilon[x]} \left(\max_{j \neq y} (f_\theta^j(\tilde{x}) - f_\theta^y(\tilde{x}) - \kappa, 0) \right), \quad (2)$$

where κ is a positive constant value that aids the optimization. When the logit margin is small and close to 0, the starting point of optimization of the inner loss of the C&W attack (i.e., $(\max_{j \neq y} (f_\theta^j(\tilde{x}) - f_\theta^y(\tilde{x}) - \kappa, 0))$ in Eq. (2)) is also small and close to 0. This will incur the gradient vanishing problem and hurdle the optimization for finding the C&W-adversarial data. Therefore, NL in outer minimization obfuscates gradients of C&W attacks by reducing logit margins.

In Section 3, we have investigated NL injection in inner maximization for benefiting generalization. In Section 4, we have investigated NL injection in outer minimization for benefiting robustness. When injecting NL in both inner maximization and outer minimization, we found that the performance is very similar to (even slightly better than) NL injection in outer minimization. We leave those results for Appendix C. In the following section, we will design our method to inject NL automatically. Our simple strategy can benefit various AT methods.

5 Algorithm, Experiment and Further Analysis

In Section 5.1, we propose an automatic NL injection strategy to unleash the full power of NL injection to combat the robust overfitting and enhance the adversarial robustness. In Section 5.2, we provide further analyses and conduct ablation studies of NL injection.

5.1 NoiLIn: An Automatic NL Injection Strategy

For benefiting adversarial robustness, we propose a simple NL injection strategy that gradually increases the rate of NL injection (i.e., NoiLIn in Algorithm 1). At each training epoch, we randomly flip η portion of labels of training dataset S_{train} to get a noisy dataset \tilde{S} ; then, we conduct existing AT methods (e.g., standard AT [20] and TRADES [42]) using the noisy dataset \tilde{S} . We monitor the training process using a clean validation

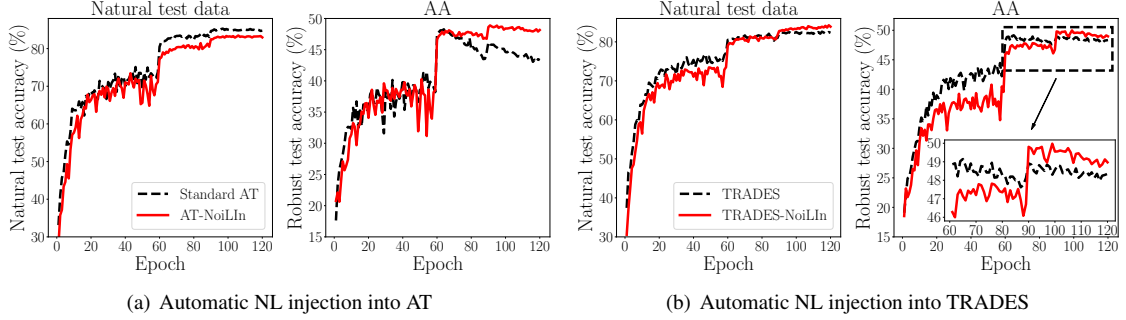


Figure 6: Evaluations on ResNet-18. We compared generalization and robustness between our NoiLIn (Algorithm 1, red lines) and two typical methods such as standard AT and TRADES (black lines). We leave the robustness evaluated by PGD-40 attack and C&W $_{\infty}$ -30 attack for Appendix D.2.

Table 1: Evaluations on Wide ResNet. We reported the test accuracy of the best checkpoint and that of the last checkpoint as well as the gap between them—“best/last (gap)”.

Defense	Natural	C&W $_{\infty}$ -100	AA
Standard AT [20]	87.00/87.13 (+0.13)	53.47/46.75 (-6.72)	51.06/45.29 (-5.77)
AT-NoiLIn	85.92/86.43 (+0.51)	55.99/53.79 (-2.20)	52.50/50.62 (-1.88)
TRADES [42]	84.92/85.16 (+0.25)	53.69/49.89 (-3.80)	52.54/47.95 (-4.59)
TRADES-NoiLIn	84.39/ 85.89 (+1.50)	54.37/51.69 (-2.68)	53.14/50.16 (-2.88)

set. We increase noise injection rate η by a small ratio γ during the training process once robust overfitting occurs.

In Figure 6 (using ResNet-18) and Table 1 (using Wide ResNet [39]), we compared our Algorithm 1 with two typical AT methods, i.e., standard AT [20] and TRADES [42] using CIFAR-10 dataset. We took 1000 data from training set for validation and took the remaining data for the learning. The robust validation accuracy (\mathcal{A}_e in Algorithm 1) was evaluated on PGD-10 attack for the consideration of speed. For the hyperparameter setting of AT-NoiLIn, the noise rate η was initialized as $\eta_{\min} = 0.05$ with $\eta_{\max} = 0.3$, $\tau = 10$ and $\gamma = 0.1$. For the hyperparameter setting of TRADES-NoiLIn, we set $\eta_{\min} = 0.05$, $\eta_{\max} = 0.2$, $\tau = 10$ and $\gamma = 0.05$. Other settings (e.g., learning rate, optimizer) kept the same as Section 3.1. Note that in Table 1, we used WRN-32-10 for AT-NoiLIn and WRN-34-10 for TRADES-NoiLIn that kept same as [20] and [42], respectively. In Figure 6 and Table 1, we injected symmetric-flipping NL and deferred the results of pair-flipping NL to Appendix D.3. In addition, we also conducted Algorithm 1 on SVHN [23] dataset in Appendix D.4.

Figure 6 demonstrates the learning curves of NoiLIn (red lines) and two typical AT methods on ResNet-18 (black lines). Figure 6 shows that the robust test accuracy of NoiLIn keeps steady and even rises slightly instead of immediately dropping when the learning rate decays. In Table 1, we reported the robustness evaluations on Wide ResNet and reported the best checkpoint, the last checkpoint and the gap between them. The best checkpoints were selected based on PGD-10 attack when using Wide ResNet, and the detailed selection metric for the best checkpoints was illustrated in Appendix D.1. Table 1 shows that NoiLIn can clearly narrow the gap between the robustness of the best checkpoint and that of the last checkpoint; NoiLIn can even boost robustness of the best checkpoint. Therefore, our simple yet effective strategy can mitigate robust overfitting and enhance adversarial robustness.

5.2 Further Analysis and Ablation Study

In this section, we show AT-NoiLIn is less sensitive to weight decay than standard AT, and we compare AT-NoiLIn with the technique of label smoothing (LS). In addition, we conduct extensive ablation studies such as NoiLIn with various learning rate schedulers, various perturbation bounds ϵ and various noisy-label training set.

Sensitivity to weight decay. Pang et al. [25] empirically found different values of weight decay can largely affect AT’s adversarial robustness. In Proposition 1 (in Appendix A), we found NL injection can implicitly

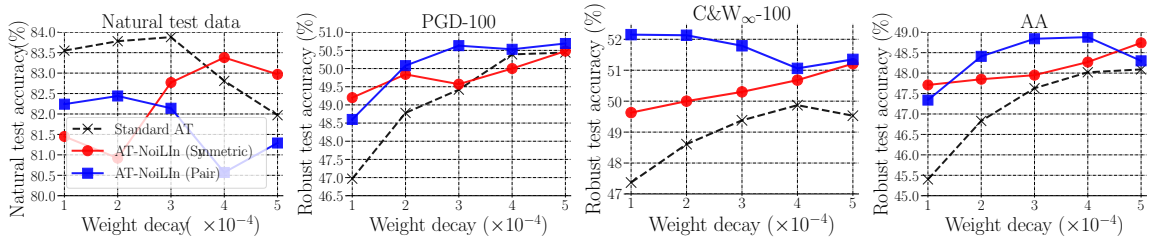


Figure 7: Test accuracy of robust models trained under different values of weight decay. We abbreviate AT-NoiLIn using symmetric-flipping NL as “AT-NoiLIn (Symmetric)” and AT-NoiLIn using pair-flipping NL as “AT-NoiLIn (Pair)”.

Table 2: Comparisons between standard AT, AT-LS ($\rho = 0.1$) and AT-NoiLIn (Symmetric). We reported the test accuracy of the best checkpoint and that of the last checkpoint as well as the gap between them—“best/last (gap)”.

Defense	Natural	C&W $_{\infty}$ -100	AA
Standard AT [20]	81.97/84.76 (+2.79)	49.53/45.12 (-4.71)	48.09/43.30 (-4.79)
AT-LS [25]	82.76/ 85.15 (+2.39)	50.06/45.40 (-4.66)	48.60/43.44 (-5.16)
AT-NoiLIn	82.97 /83.86 (+0.89)	51.21/50.36 (-0.85)	48.74/47.93 (-0.81)

penalize the magnitude of model parameters, which has a similar effect of weight decay. Proposition 1 intrigued us to explore the sensitivity of AT with NL to weight decay.

In Figure 7, we conducted Algorithm 1 under different values of weight decay and compared the Algorithm 1 with standard AT. We used ResNet-18 and evaluated robustness at the best checkpoint. The settings kept the same as [25]. From the right three panels of Figure 7, both red and blue lines are higher and flatter than black lines across different values of weight decay. It signifies that noise injection can enhance adversarial robustness and meanwhile make AT less sensitive to varying values of weight decay.

Relation with label smoothing (LS). When taking the expectation w.r.t. all training epochs, NL injection is similar to employing the technique of label smoothing into AT (AT-LS) [10, 25]. Despite the mathematical similarity, we show that AT-NoiLIn has advantages over AT-LS in terms of a) relieving robust overfitting and b) computational efficiency.

AT-LS uses the ρ level of smoothed label \bar{y} in outer minimization while using the one-hot label y in inner maximization. The ρ level of smoothed label \bar{y} is a C -dimensional vector with the y -th dimension being $1 - \rho$ and all others being $\frac{\rho}{C-1}$.

In Table 2, we reported robustness evaluations of AT-LS ($\rho = 0.1$) and AT-NoiLIn using ResNet-18 on CIFAR-10 dataset and set training details same as Section 5.1. Comparisons between AT-LS under other different ρ and AT-NoiLIn are reported in Appendix E. Table 2 shows that compared with standard AT, AT-NoiLIn can largely relieve robust overfitting, while AT-LS fails to make any effect. The reasons may be that AT-LS uses fixed smoothed labels, which is similar to AT using fixed one-hot labels, thereby incurring lower data variance during the training process; by contrast, AT-NoiLIn randomly flips labels at each epoch, leading to higher data variance and thus preventing robust overfitting (justified in Section 4.2).

In addition, AT-NoiLIn is more computationally efficient than AT-LS. For each adversarial training data \tilde{x} whose prediction is $p(\tilde{x})$, the calculation of the cross-entropy loss of AT-LS is $-\sum_{j=1}^C \bar{y}_j \log p_j(\tilde{x})$ while that of AT-NoiLIn is $-\log p_{\bar{y}}(\tilde{x})$. AT-NoiLIn saves $(C - 1)$ log operations for each data. We discuss the empirical verification on this claim in Appendix E.

NoiLIn under different learning rate (LR) schedulers. Rice et al. [27] showed robust overfitting occurs in AT under different LR schedulers. In Appendix F, we conducted AT-NoiLIn under different LR schedulers, which justifies that AT-NoiLIn can still relieve robust overfitting under different LR schedulers (Figure 13 and Table 5).

NoiLIn under larger ϵ_{train} . In Appendix G, we conducted AT-NoiLIn under larger ϵ_{train} and showed robustness evaluations under $\epsilon_{\text{test}} = \epsilon_{\text{train}}$. When ϵ_{train} becomes larger (e.g., $\epsilon_{\text{train}} > 8/255$ in CIFAR-10),

our AT-NoiLIn can mitigate robust overfitting and significantly improve the robust test accuracy compared with standard AT methods (Figures 14 and 15).

NoiLIn under noisy-label training set. In practice, training set is often intrinsically noisy-label due to expensive and time-consuming annotations [37]. In Appendix H, we compared AT-NoiLIn with standard AT on noisy-label versions of CIFAR-10 dataset. Figure 16 shows the larger noisy-label training set can indeed cause larger performance degradation in both AT-NoiLIn and standard AT. Interestingly, compared with standard AT, our AT-NoiLIn has better performance in both generalization and robustness across various noisy-label sets. The reason may be that AT-NoiLIn randomly flips labels over the training process, which makes the training less likely to be overconfident on the wrongly annotated labels.

6 Conclusion

In this paper, we claim that NL can benefit AT. We have explored the positive effects of NL injection in inner maximization and in outer minimization, respectively. Our observations have motivated us to propose a simple but effective strategy, namely “NoiLIn”, to combat the issue of robust overfitting and enhance robustness further.

There are two limitations of our current work. 1) We empirically verified the benefits of NoiLIn, but it is still difficult to explicitly, not intuitively, explain why NL injection improves robustness. 2) We do not know the optimal rate of NL injection at each training epoch, except leveraging validation set. In the future, we will attempt to address these limitations.

Acknowledgement

JZ, GN, and MS were supported by JST AIP Acceleration Research Grant Number JPMJCR20U3, Japan. MS was also supported by the Institute for AI and Beyond, UTokyo. BH was supported by the RGC Early Career Scheme No. 22200720 and NSFC Young Scientists Fund No. 62006202. TL was supported by Australian Research Council Project DE-190101473. LC was supported by the NSFC No.91846205.

References

- [1] Jean-Baptiste Alayrac, Jonathan Uesato, Po-Sen Huang, Alhussein Fawzi, Robert Stanforth, and Pushmeet Kohli. Are labels required for improving adversarial robustness? In *NeurIPS*, 2019.
- [2] Dana Angluin and Philip Laird. Learning from noisy examples. *Machine Learning*, 2(4):343–370, 1988.
- [3] Devansh Arpit, Stanisław Jastrzębski, Nicolas Ballas, David Krueger, Emmanuel Bengio, Maxinder S Kanwal, Tegan Maharaj, Asja Fischer, Aaron Courville, Yoshua Bengio, et al. A closer look at memorization in deep networks. In *ICML*, 2017.
- [4] Anish Athalye, Nicholas Carlini, and David A. Wagner. Obfuscated gradients give a false sense of security: Circumventing defenses to adversarial examples. In *ICML*, 2018.
- [5] Vivek B.S. and R. Venkatesh Babu. Single-step adversarial training with dropout scheduling. In *CVPR*, 2020.
- [6] Qi-Zhi Cai, Chang Liu, and Dawn Song. Curriculum adversarial training. In *IJCAI*, 2018.
- [7] Nicholas Carlini and David A. Wagner. Towards evaluating the robustness of neural networks. In *Symposium on Security and Privacy (SP)*, 2017.
- [8] Yair Carmon, Aditi Raghunathan, Ludwig Schmidt, Percy Liang, and John C. Duchi. Unlabeled data improves adversarial robustness. In *NeurIPS*, 2019.
- [9] Tianlong Chen, Zhenyu Zhang, Sijia Liu, Shiyu Chang, and Zhangyang Wang. Robust overfitting may be mitigated by properly learned smoothing. In *ICLR*, 2021.
- [10] Minhao Cheng, Qi Lei, Pin-Yu Chen, Inderjit Dhillon, and Cho-Jui Hsieh. Cat: Customized adversarial training for improved robustness. *arXiv:2002.06789*, 2020.
- [11] Francesco Croce and Matthias Hein. Reliable evaluation of adversarial robustness with an ensemble of diverse parameter-free attacks. In *ICML*, 2020.
- [12] Jia Deng, Wei Dong, Richard Socher, Li-Jia Li, Kai Li, and Li Fei-Fei. Imagenet: A large-scale hierarchical image database. In *2009 IEEE conference on computer vision and pattern recognition*, pages 248–255. Ieee, 2009.
- [13] Gavin Weiguang Ding, Yash Sharma, Kry Yik Chau Lui, and Ruitong Huang. Mma training: Direct input space margin maximization through adversarial training. In *ICLR*, 2020.
- [14] Ian J. Goodfellow, Jonathon Shlens, and Christian Szegedy. Explaining and harnessing adversarial examples. In *ICLR*, 2015.
- [15] Bo Han, Jiangchao Yao, Gang Niu, Mingyuan Zhou, Ivor W. Tsang, Ya Zhang, and Masashi Sugiyama. Masking: A new perspective of noisy supervision. In *NeurIPS*, 2018.
- [16] Bo Han, Quanming Yao, Xingrui Yu, Gang Niu, Miao Xu, Weihua Hu, Ivor Tsang, and Masashi Sugiyama. Co-teaching: Robust training of deep neural networks with extremely noisy labels. In *NeurIPS*, 2018.
- [17] Kaiming He, Xiangyu Zhang, Shaoqing Ren, and Jian Sun. Deep residual learning for image recognition. In *CVPR*, 2016.
- [18] Lu Jiang, Zhengyuan Zhou, Thomas Leung, Li-Jia Li, and Li Fei-Fei. Mentornet: Learning data-driven curriculum for very deep neural networks on corrupted labels. In *ICML*, 2018.
- [19] Alex Krizhevsky. Learning multiple layers of features from tiny images. Technical report, 2009.
- [20] Aleksander Madry, Aleksandar Makelov, Ludwig Schmidt, Dimitris Tsipras, and Adrian Vladu. Towards deep learning models resistant to adversarial attacks. In *ICLR*, 2018.

- [21] Amir Najafi, Shin-ichi Maeda, Masanori Koyama, and Takeru Miyato. Robustness to adversarial perturbations in learning from incomplete data. In *NeurIPS*, 2019.
- [22] Nagarajan Natarajan, Inderjit S Dhillon, Pradeep K Ravikumar, and Ambuj Tewari. Learning with noisy labels. In *NeurIPS*, 2013.
- [23] Yuval Netzer, Tao Wang, Adam Coates, Alessandro Bissacco, Bo Wu, and Andrew Y Ng. Reading digits in natural images with unsupervised feature learning. In *NeurIPS Workshop on Deep Learning and Unsupervised Feature Learning*, 2011.
- [24] Duc Tam Nguyen, Chaithanya Kumar Mummadi, Thi Phuong Nhung Ngo, Thi Hoai Phuong Nguyen, Laura Beggel, and Thomas Brox. Self: Learning to filter noisy labels with self-ensembling. In *ICLR*, 2019.
- [25] Tianyu Pang, Xiao Yang, Yinpeng Dong, Hang Su, and Jun Zhu. Bag of tricks for adversarial training. *ICLR*, 2021.
- [26] Giorgio Patrini, Alessandro Rozza, Aditya Krishna Menon, Richard Nock, and Lizhen Qu. Making deep neural networks robust to label noise: A loss correction approach. In *CVPR*, 2017.
- [27] Leslie Rice, Eric Wong, and J Zico Kolter. Overfitting in adversarially robust deep learning. In *ICML*, 2020.
- [28] Amartya Sanyal, Puneet K. Dokania, Varun Kanade, and Philip Torr. How benign is benign overfitting ? In *ICLR*, 2021.
- [29] Ali Shafahi, Mahyar Najibi, Mohammad Amin Ghiasi, Zheng Xu, John Dickerson, Christoph Studer, Larry S Davis, Gavin Taylor, and Tom Goldstein. Adversarial training for free! In *NeurIPS*, 2019.
- [30] Christian Szegedy, Wojciech Zaremba, Ilya Sutskever, Joan Bruna, Dumitru Erhan, Ian Goodfellow, and Rob Fergus. Intriguing properties of neural networks. In *ICLR*, 2014.
- [31] Brendan Van Rooyen, Aditya Krishna Menon, and Robert C Williamson. Learning with symmetric label noise: The importance of being unhinged. In *NeurIPS*, 2015.
- [32] Yisen Wang, Xingjun Ma, James Bailey, Jinfeng Yi, Bowen Zhou, and Quanquan Gu. On the convergence and robustness of adversarial training. In *ICML*, 2019.
- [33] Yisen Wang, Difan Zou, Jinfeng Yi, James Bailey, Xingjun Ma, and Quanquan Gu. Improving adversarial robustness requires revisiting misclassified examples. In *ICLR*, 2020.
- [34] Eric Wong, Leslie Rice, and J. Zico Kolter. Fast is better than free: Revisiting adversarial training. In *ICLR*, 2020.
- [35] Dongxian Wu, Shu-Tao Xia, and Yisen Wang. Adversarial weight perturbation helps robust generalization. *NeurIPS*, 33, 2020.
- [36] Xiaobo Xia, Tongliang Liu, Bo Han, Nannan Wang, Mingming Gong, Haifeng Liu, Gang Niu, Dacheng Tao, and Masashi Sugiyama. Part-dependent label noise: Towards instance-dependent label noise. In *NeurIPS*, 2020.
- [37] Tong Xiao, Tian Xia, Yi Yang, Chang Huang, and Xiaogang Wang. Learning from massive noisy labeled data for image classification. In *CVPR*, 2015.
- [38] Yao-Yuan Yang, Cyrus Rashtchian, Hongyang Zhang, Russ R. Salakhutdinov, and Kamalika Chaudhuri. A closer look at accuracy vs. robustness. In *NeurIPS*, 2020.
- [39] Sergey Zagoruyko and Nikos Komodakis. Wide residual networks. *arXiv:1605.07146*, 2016.
- [40] Chiyuan Zhang, Samy Bengio, Moritz Hardt, Benjamin Recht, and Oriol Vinyals. Understanding deep learning requires rethinking generalization. In *ICLR*, 2017.

- [41] Dinghuai Zhang, Tianyuan Zhang, Yiping Lu, Zhanxing Zhu, and Bin Dong. You only propagate once: Accelerating adversarial training via maximal principle. In *NeurIPS*, 2019.
- [42] Hongyang Zhang, Yaodong Yu, Jiantao Jiao, Eric P. Xing, Laurent El Ghaoui, and Michael I. Jordan. Theoretically principled trade-off between robustness and accuracy. In *ICML*, 2019.
- [43] Jingfeng Zhang, Xilie Xu, Bo Han, Gang Niu, Lizhen Cui, Masashi Sugiyama, and Mohan Kankanhalli. Attacks which do not kill training make adversarial learning stronger. In *ICML*, 2020.
- [44] Jingfeng Zhang, Jianing Zhu, Gang Niu, Bo Han, Masashi Sugiyama, and Mohan Kankanhalli. Geometry-aware instance-reweighted adversarial training. In *ICLR*, 2021.
- [45] Jianing Zhu, Jingfeng Zhang, Bo Han, Tongliang Liu, Gang Niu, Hongxia Yang, Mohan Kankanhalli, and Masashi Sugiyama. Understanding the interaction of adversarial training with noisy labels. *arXiv:2102.03482*, 2021.

A Proof of Proposition 1

Proposition 1. For any classifier $f_\theta : \mathcal{X} \rightarrow \mathcal{Y}$ with classifier parameters θ , intact dataset D on $\mathcal{X} \times \mathcal{Y}$, noisy dataset \tilde{D} on $\mathcal{X} \times \tilde{\mathcal{Y}}$, noisy label set $\tilde{\mathcal{Y}}$ is generated by randomly flipping η portion of intact labels from intact label set \mathcal{Y} , adversarial risk on intact dataset D is defined by [42] as $\mathcal{R}_{\text{rob}}(f_\theta, D) := \mathbb{E}_{(X,Y) \sim D} \mathbb{1}\{\exists X' \in \mathcal{B}_\epsilon[X] : f_\theta(X') \neq Y\}$, the classifier minimizes the following risk on noisy dataset \tilde{D} :

$$\min_{\theta} \mathcal{R}_{\text{rob}}(f_\theta, \tilde{D}) := \mathbb{E}_{(X,\tilde{Y}) \sim \tilde{D}} \mathbb{1}\{\exists X' \in \mathcal{B}_\epsilon[X] : f_\theta(X') \neq \tilde{Y}\} \quad (3)$$

and

$$\eta \cdot (1 - 2 \cdot \mathcal{R}_{\text{rob}}(f_\theta, D)) \leq \mathcal{R}_{\text{rob}}(f_\theta, \tilde{D}) - \mathcal{R}_{\text{rob}}(f_\theta, D) \leq \eta \cdot (1 - \mathcal{R}_{\text{rob}}(f_\theta, D)). \quad (4)$$

Proof. We first derive the lower bound of $\mathcal{R}_{\text{rob}}(f_\theta, \tilde{D})$.

$$\begin{aligned} \mathcal{R}_{\text{rob}}(f_\theta, \tilde{D}) &:= \mathbb{E}_{(X,\tilde{Y}) \sim \tilde{D}} \mathbb{1}\{\exists X' \in \mathcal{B}_\epsilon[X] : f_\theta(X') \neq \tilde{Y}\} \\ &= \mathbb{E}_{\tilde{Y} \sim \tilde{\mathcal{Y}}, Y \sim \mathcal{Y}} (\mathbb{1}\{\tilde{Y} \neq Y\}) \cdot \mathbb{E}_{(X,Y) \sim D} (\mathbb{1}\{\exists X' \in \mathcal{B}_\epsilon[X], \exists Y' \in (\mathcal{Y} - \tilde{\mathcal{Y}}) : f_\theta(X') = Y'\}) \\ &\quad + \mathbb{E}_{\tilde{Y} \sim \tilde{\mathcal{Y}}, Y \sim \mathcal{Y}} (\mathbb{1}\{\tilde{Y} = Y\}) \cdot \mathbb{E}_{(X,Y) \sim D} (\mathbb{1}\{\exists X' \in \mathcal{B}_\epsilon[X] : f_\theta(X') \neq Y\}) \end{aligned} \quad (5)$$

$$\begin{aligned} &\geq \mathbb{E}_{\tilde{Y} \sim \tilde{\mathcal{Y}}, Y \sim \mathcal{Y}} (\mathbb{1}\{\tilde{Y} \neq Y\}) \cdot \mathbb{E}_{(X,Y) \sim D} (\mathbb{1}\{\exists X' \in \mathcal{B}_\epsilon[X] : f_\theta(X') = Y\}) \\ &\quad + \mathbb{E}_{\tilde{Y} \sim \tilde{\mathcal{Y}}, Y \sim \mathcal{Y}} (\mathbb{1}\{\tilde{Y} = Y\}) \cdot \mathbb{E}_{(X,Y) \sim D} (\mathbb{1}\{\exists X' \in \mathcal{B}_\epsilon[X] : f_\theta(X') \neq Y\}) \end{aligned} \quad (6)$$

$$\begin{aligned} &= \eta \cdot (1 - \mathbb{E}_{(X,Y) \sim D} (\mathbb{1}\{\exists X' \in \mathcal{B}_\epsilon[X] : f_\theta(X') \neq Y\})) \\ &\quad + (1 - \eta) \cdot \mathbb{E}_{(X,Y) \sim D} (\mathbb{1}\{\exists X' \in \mathcal{B}_\epsilon[X] : f_\theta(X') \neq Y\}) \end{aligned} \quad (7)$$

$$= \eta \cdot (1 - \mathcal{R}_{\text{rob}}(f_\theta, D)) + (1 - \eta) \cdot \mathcal{R}_{\text{rob}}(f_\theta, D) \quad (8)$$

$$= \mathcal{R}_{\text{rob}}(f_\theta, D) + \eta \cdot (1 - 2 \cdot \mathcal{R}_{\text{rob}}(f_\theta, D)) \quad (9)$$

The upper bound of $\mathcal{R}_{\text{rob}}(f_\theta, \tilde{D})$ is derived as follows.

$$\begin{aligned} \mathcal{R}_{\text{rob}}(f_\theta, \tilde{D}) &:= \mathbb{E}_{(X,\tilde{Y}) \sim \tilde{D}} \mathbb{1}\{\exists X' \in \mathcal{B}_\epsilon[X] : f_\theta(X') \neq \tilde{Y}\} \\ &= \mathbb{E}_{\tilde{Y} \sim \tilde{\mathcal{Y}}, Y \sim \mathcal{Y}} (\mathbb{1}\{\tilde{Y} \neq Y\}) \cdot \mathbb{E}_{(X,Y) \sim D} (\mathbb{1}\{\exists X' \in \mathcal{B}_\epsilon[X], \exists Y' \in (\mathcal{Y} - \tilde{\mathcal{Y}}) : f_\theta(X') = Y'\}) \\ &\quad + \mathbb{E}_{\tilde{Y} \sim \tilde{\mathcal{Y}}, Y \sim \mathcal{Y}} (\mathbb{1}\{\tilde{Y} = Y\}) \cdot \mathbb{E}_{(X,Y) \sim D} (\mathbb{1}\{\exists X' \in \mathcal{B}_\epsilon[X] : f_\theta(X') \neq Y\}) \end{aligned} \quad (10)$$

$$\begin{aligned} &\leq \mathbb{E}_{\tilde{Y} \sim \tilde{\mathcal{Y}}, Y \sim \mathcal{Y}} (\mathbb{1}\{\tilde{Y} \neq Y\}) \cdot \mathbb{E}_{(X,Y) \sim D} (\mathbb{1}\{\exists X' \in \mathcal{B}_\epsilon[X], \exists Y' \in \mathcal{Y} : f_\theta(X') = Y'\}) \\ &\quad + \mathbb{E}_{\tilde{Y} \sim \tilde{\mathcal{Y}}, Y \sim \mathcal{Y}} (\mathbb{1}\{\tilde{Y} = Y\}) \cdot \mathbb{E}_{(X,Y) \sim D} (\mathbb{1}\{\exists X' \in \mathcal{B}_\epsilon[X] : f_\theta(X') \neq Y\}) \end{aligned} \quad (11)$$

$$= \eta + (1 - \eta) \cdot \mathbb{E}_{(X,Y) \sim D} (\mathbb{1}\{\exists X' \in \mathcal{B}_\epsilon[X] : f_\theta(X') \neq Y\}) \quad (12)$$

$$= \eta + (1 - \eta) \cdot \mathcal{R}_{\text{rob}}(f_\theta, D) \quad (13)$$

$$= \mathcal{R}_{\text{rob}}(f_\theta, D) + \eta \cdot (1 - \mathcal{R}_{\text{rob}}(f_\theta, D)) \quad (14)$$

Therefore, according to Eq. (9) and Eq. (14), we have

$$\eta \cdot (1 - 2 \cdot \mathcal{R}_{\text{rob}}(f_\theta, D)) \leq \mathcal{R}_{\text{rob}}(f_\theta, \tilde{D}) - \mathcal{R}_{\text{rob}}(f_\theta, D) \leq \eta \cdot (1 - \mathcal{R}_{\text{rob}}(f_\theta, D)).$$

Eq. (5) and Eq. (10) come from the fact $\Pr[f(X') \neq \tilde{Y}] = \Pr[\tilde{Y} \neq Y, f(X') \in (\mathcal{Y} - \tilde{\mathcal{Y}})] \cup \Pr[\tilde{Y} = Y, f(X') \neq Y]$. Eq. (6) and Eq. (11) come from $\Pr[\tilde{Y} \neq Y, f(X') = Y \in (\mathcal{Y} - \tilde{\mathcal{Y}})] \subseteq \Pr[\tilde{Y} \neq Y, f(X') \in (\mathcal{Y} - \tilde{\mathcal{Y}})] \subseteq \Pr[\tilde{Y} \neq Y, f(X') \in \mathcal{Y}]$. Eq. (7) and Eq. (12) hold by the equation $\mathbb{E}_{\tilde{Y} \sim \tilde{\mathcal{Y}}, Y \sim \mathcal{Y}} (\mathbb{1}\{\tilde{Y} \neq Y\}) = \eta$. Eq. (8) and Eq. (13) hold by the equation $\mathcal{R}_{\text{rob}}(f_\theta, D) := \mathbb{E}_{(X,Y) \sim D} \mathbb{1}\{\exists X' \in \mathcal{B}_\epsilon[X] : f_\theta(X') \neq Y\}$. \square

In Proposition 1, we theoretically prove adversarial risk on noisy dataset is a regularized adversarial risk with regularization term at least $\eta \cdot (1 - 2 \cdot \mathcal{R}_{\text{rob}}(f_\theta, D))$, which we call NL regularization \mathcal{R}_{NL} . Note that when $\eta = 0$, $\mathcal{R}_{\text{rob}}(f_\theta, \tilde{D})$ is exactly same as $\mathcal{R}_{\text{rob}}(f_\theta, D)$. When $\eta > 0$ and $\mathcal{R}_{\text{rob}}(f_\theta, D) < 1/2$, $\mathcal{R}_{\text{NL}} > 0$ is an implicit regularization that adds penalty on the magnitude of model parameters. Weight decay is a regularization that directly adds ℓ_2 penalty ($\frac{1}{2}\omega\|\theta\|_2^2$) on model parameters where ω is the value of weight decay. Therefore, the effect of \mathcal{R}_{NL} might be similar to that of weight decay, thus making AT less sensitive to varying values of weight decay (validated in Section 5.2).

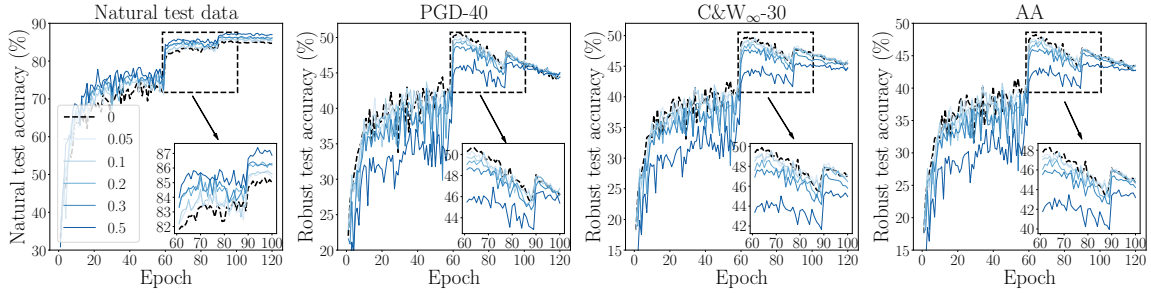
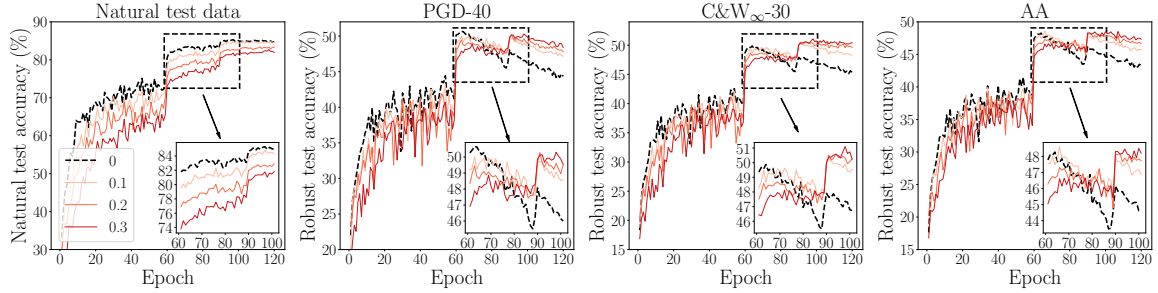
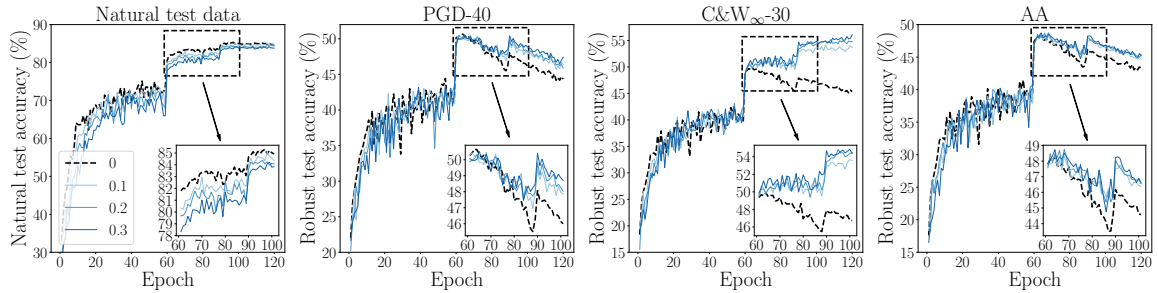


Figure 8: The learning curves of injecting various levels of pair-flipping NL in inner maximization. The number in the legend represents noise rate η .



(a) Symmetric-flipping NL



(b) Pair-flipping NL

Figure 9: The learning curves of injecting various levels of on-the-fly NL into both inner maximization and outer minimization. The number in the legend represents noise rate η .

B Injecting Pair-flipping NL in Inner Maximization

We showed the performance of AT with pair-flipping NL injection in inner maximization (blue lines with different shades) in Figure 8, which indicates NL injection in inner maximization can improve natural generalization. Training details of AT with pair-flipping NL injection in inner maximization kept same as Section 3.1. Observed from Figure 8, mild portion of pair-flipping NL injection in inner maximization (e.g., $\eta \leq 0.3$) benefits AT’s natural generalization while hardly hurting robustness. Therefore, we empirically justified NL injection in inner maximization improves generalization.

C Injecting NL in Both Inner Maximization and Outer Minimization

We reported the learning curves of ResNet-18 trained by AT with NL injection in inner maximization and outer minimization simultaneously on CIFAR-10 dataset in Figure 9(a) (symmetric-flipping NL) and Figure 9(b) (pair-flipping NL). The noise rate η was sampled from $\{0.1, 0.2, 0.3\}$. The detailed training settings (e.g., the optimizer and learning schedule) were the same as Section 3.1.

Figures 9(a) and 9(b) show that, with the increasing of η (the color gradually becomes deeper), the standard test accuracy (the leftmost panels) on natural test data decreases ; while the robust test accuracy (the right three panels) on adversarial data evaluated at the last checkpoint and at the best checkpoint increases simultaneously.

For example, when η equals to 0.1 (blue lines with different shades) in Figure 9(a), the standard test accuracy at Epoch 120 is comparable with standard AT (black dashed line), and the robust test accuracy at Epoch 120 is obviously above the black dashed line. Such observation manifests that injecting NL in both inner maximization and outer minimization can alleviate robust overfitting, thus further improving adversarial robustness, which validates that NL is not always harmful to AT.

D Extensive Experimental Details and Evaluations of NoiLin

In this section, we state more experimental details, such as the computing resources and the selection metric for the best checkpoint, and demonstrate extensive evaluations of our NoiLin framework.

D.1 More Experimental Details

Computing resources. All experiments were conducted on a machine with Intel Xeon Gold 5218 CPU, 250GB RAM and six NVIDIA Tesla V100 SXM2 GPU, and three machines with Intel Xeon Silver 4214 CPU, 128GB RAM and four GeForce RTX 2080 Ti GPU.

Selection metric for the best checkpoint. We selected the best checkpoint based on robust test accuracy on AA [11] adversarial data when using ResNet-18, and PGD-10 adversarial data when using Wide ResNet for the consideration of speed. Note that we reported the evaluations at the best checkpoint in Figure 7, Figure 15, Figure 16, and all tables.

A confusing phenomenon occurs that the natural test accuracy shown in the learning curve figure (e.g., Figure 6(a)) is seemingly inconsistent with that evaluated at the best checkpoint (e.g., Table 2). In the left panel of Figure 6(a), the natural test accuracy of AT-NoiLin (Symmetric) is lower than that of standard AT at every epoch. By contrast, in Table 2, the natural test accuracy of AT-NoiLin (Symmetric) evaluated at the best checkpoint is 82.97%, which is higher than that of standard AT (81.97%).

This contradiction is owing to that we reported the test accuracy of standard AT and AT-NoiLin (Symmetric) at the epoch when the model gained the most robustness against AA attacks in Table 2. In detail, the best checkpoint of standard AT was selected at Epoch 63 while that of AT-NoiLin (Symmetric) was selected at Epoch 96. Therefore, despite that the red line is consistently below the black line in the left panel of Figure 6(a), the natural test accuracy of AT-NoiLin (Symmetric) reported in Table 2 is evaluated at Epoch 96, which is higher than that of standard AT evaluated at Epoch 63.

Similarly, when $\epsilon = 16/255$, the best checkpoint of standard AT was selected at Epoch 89 while that of AT-NoiLin (Pair) was selected at Epoch 102. The natural test accuracy of standard AT under $\epsilon_{\text{train}} = 16/255$ at Epoch 89 is 66.54% while that of AT-NoiLin (Pair) under $\epsilon_{\text{train}} = 16/255$ is 66.72%. Therefore, in spite of the blue line (AT-NoiLin (Pair)) being always below the black line (standard AT) in the leftmost panel of Figure 14, the blue pillar (AT-NoiLin (Pair)) is comparable with the black pillar (standard AT) in the leftmost panel of Figure 15 when $\epsilon = 16/255$.

D.2 Extensive Evaluations of NoiLin Using Symmetric-flipping NL

We demonstrated robustness evaluations based on PGD-40 attack and C&W $_{\infty}$ -30 attack of AT-NoiLin (Symmetric) in Figure 10(a) and TRADES-NoiLin (Symmetric) in Figure 10(b). Figure 10 suggests our NoiLin framework can largely combat the issue of robust overfitting and further enhance adversarial robustness.

D.3 Robustness Evaluations of NoiLin Using Pair-flipping NL

We compared the NoiLin framework using pair-flipping NL with two conventional AT methods, i.e., standard AT and TRADES. We reported the learning curves on ResNet-18 in Figure 11 and robustness evaluations on Wide ResNet in Table 3. The training details (e.g., optimizer, learning rate schedule) of AT-NoiLin using pair-flipping NL and TRADES-NoiLin using pair-flipping NL kept exactly same as Section 5.1.

In the right three panels of Figure 11(a), we observed the robust test accuracy of AT-NoiLin (blue lines) consistently exceeds that of standard AT (black lines) after the learning rate decays. In Table 3, we found the

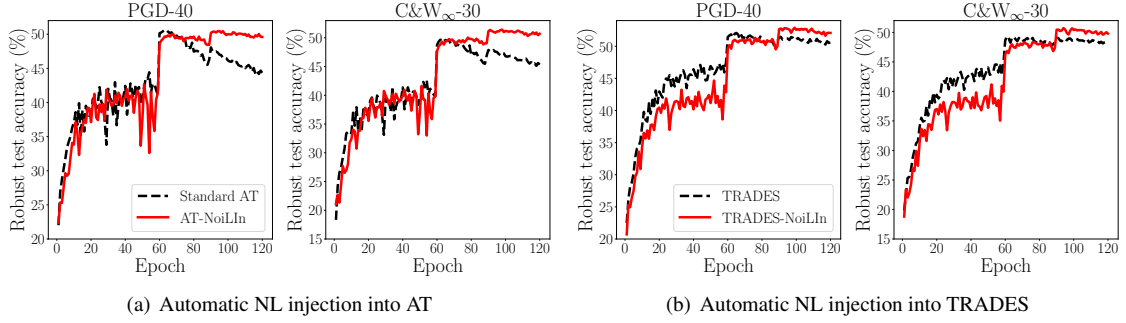
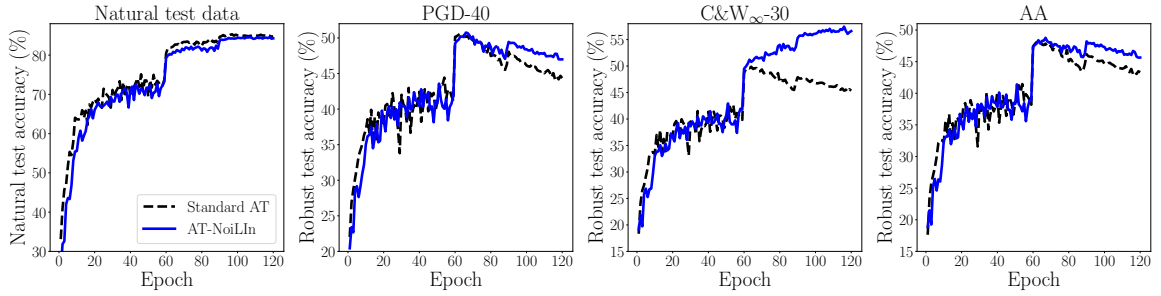
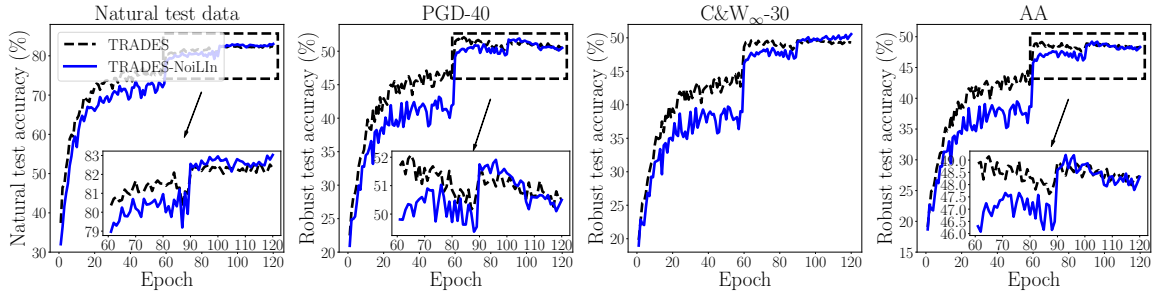


Figure 10: Evaluations on ResNet-18. We compared robustness evaluated by PGD-40 attack and $C\&W_{\infty}-30$ attack between our NoiLIn (red lines) and two typical methods such as standard AT and TRADES (black lines).



(a) Automatic NL injection into AT



(b) Automatic NL injection into TRADES

Figure 11: Evaluations on ResNet-18. We compared generalization and robustness between our NoiLIn using pair-flipping NL (blue lines) and two typical methods such as standard AT and TRADES (black lines).

absolute value of the gap (in parentheses) obtained by NoiLIn is smaller than that obtained by conventional AT methods. These discoveries indicate NoiLIn can relieve robust overfitting to a large extent.

In addition, compared with NoiLIn using symmetric-flipping NL, we found NoiLIn using pair-flipping NL can greatly enhance adversarial robustness against the C&W attack. Especially, AT-NoiLIn using Wide ResNet improves $\sim 7\%$ robust test accuracy on C&W-adversarial data compared with standard AT in Table 3. NoiLIn benefiting adversarial robustness against the C&W attack could be attributed to NL in outer minimization obfuscating gradients [4] (details in Section 4.2).

D.4 NoiLIn on SVHN Dataset

We conducted AT-NoiLIn using ResNet-18 on SVHN [23] dataset. For SVHN, the perturbation bound was set to $\epsilon_{\text{train}} = 0.031$. We set the number of PGD steps $K = 10$ and step size $\alpha = 0.003$. We trained ResNet-18 using SGD with 0.9 momentum for 120 epochs with the initial learning rate of 0.01 and divided by 10 at Epochs 60 and 90, respectively. The noise rate η was initialized as $\eta_{\text{min}} = 0.05$ with $\eta_{\text{max}} = 0.3$, $\tau = 10$ and

Table 3: Evaluations on Wide ResNet trained with NoiLIn using pair-flipping NL. We reported the test accuracy of the best checkpoint and that of the last checkpoint as well as the gap between them—“best/last (gap)”.

Defense	Natural	C&W $_{\infty}$ -100	AA
Standard AT [20]	87.00/87.13 (+0.13)	53.47/46.75 (-6.72)	51.06/45.29 (-5.77)
AT-NoiLIn	84.93/85.98 (+1.05)	54.35/63.30 (+8.95)	52.26/47.62 (-4.64)
TRADES [42]	84.92 /85.16 (+0.25)	53.69/49.89 (-3.80)	52.54/47.95 (-4.59)
TRADES-NoiLIn	84.79/ 85.95 (+1.16)	53.76/56.29 (+2.53)	52.80/50.45 (-2.35)

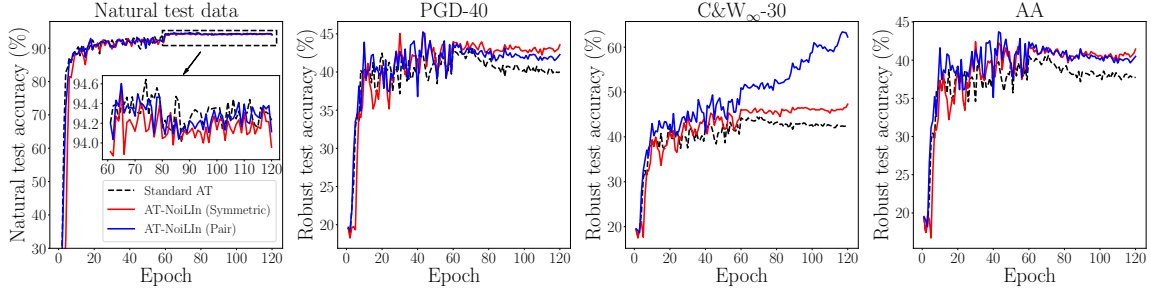


Figure 12: Evaluations on SVHN dataset. We compared generalization and robustness between our NoiLIn (both red and blue lines) and standard AT (black lines).

$\gamma = 0.05$. We took 1460 data from training set (containing 73257 training data in total) for validation and took the remaining data for the learning. The test settings (e.g., the attack methods and perturbation bound ϵ_{test}) kept same as Section 3.1. We showed the learning curves of AT-NoiLIn on SVHN dataset in Figure 12.

Figure 12 manifests AT-NoiLIn improves adversarial robustness while maintaining natural generalization. From the leftmost panel of Figure 12, we observed both blue and red lines almost align with the black line, which indicates AT-NoiLIn is not detrimental to generalization. From the right three panels, after the first learning rate decay, the black line begins to sharply drop while both red and blue lines slightly get down or even keep steady. It suggests robust overfitting occurs in AT on SVHN dataset as well, and AT-NoiLIn can also alleviate robust overfitting on SVHN dataset. Moreover, the peak performance obtained by AT-NoiLIn is clearly higher than that obtained by standard AT. Therefore, it justifies our proposed NoiLIn framework can combat issue of robust overfitting and improve robustness further.

E Relation with Label Smoothing

AT-LS [10, 25] has been comprehensively investigated among different smoothing levels ρ . Pang et al. [25] pointed out AT-LS under a mild smoothing level (e.g., $\rho = 0.1$) can slightly improve adversarial robustness. Therefore, we sampled ρ from $\{0.05, 0.1, 0.2, 0.3\}$. Training details (e.g., the optimizer and learning rate schedule) of standard AT, AT-LS under different ρ , and AT-NoiLIn (Symmetric) kept same as Section 5.1. We compared the performance of standard AT, AT-LS under different ρ , and AT-NoiLIn (Symmetric) using ResNet-18 on CIFAR-10 dataset in Table 4. We only reported AT-LS ($\rho = 0.1$) in Table 2 for the reason that AT-LS ($\rho = 0.1$) achieves the most robustness against AA attacks at the best checkpoint among AT-LS under different ρ .

AT-NoiLIn relieves robust overfitting while AT-LS does not. Compared with AT-LS under different ρ , AT-NoiLIn indeed alleviates robust overfitting. The absolute value of the robust test accuracy gap (in the parentheses at the right two columns of Table 2) obtained by AT-NoiLIn is consistently smaller than that obtained by AT-LS under different ρ . In addition, we observed AT-NoiLIn achieves better performance of robustness evaluations based on C&W attacks and AA attacks at the best epoch than AT-LS under all different ρ .

AT-NoiLIn is more computationally efficient than AT-LS. We have stated that NoiLIn saves $(C - 1)$ log operations for each data compared with LS. However, when it comes to empirical verification, we found

Table 4: Comparisons between standard AT, AT-LS under different ρ and AT-NoiLIn (Symmetric). We reported the test accuracy of the best checkpoint and that of the last checkpoint as well as the gap between them—“best/last (gap)”.

Defense	Natural	C&W $_{\infty}$ -100	AA
Standard AT [20]	81.97/84.76 (+2.79)	49.53/45.12 (-4.71)	48.09/43.30 (-4.79)
AT-LS ($\rho = 0.05$)	82.38/85.19 (+2.81)	49.60/44.95 (-4.65)	47.86/43.01 (-4.79)
AT-LS ($\rho = 0.1$)	82.76/85.15 (+2.39)	50.06/45.40 (-4.66)	48.60/43.44 (-5.16)
AT-LS ($\rho = 0.2$)	82.80/85.19 (+2.39)	49.87/45.71 (-4.16)	48.42/43.96 (-4.46)
AT-LS ($\rho = 0.3$)	82.45/ 85.70 (+3.25)	49.70/45.33 (-4.37)	48.26/43.93 (-4.33)
AT-NoiLIn (Symmetric)	82.97 /83.86 (+0.89)	51.21 / 50.36 (-0.85)	48.74 / 47.93 (-0.81)

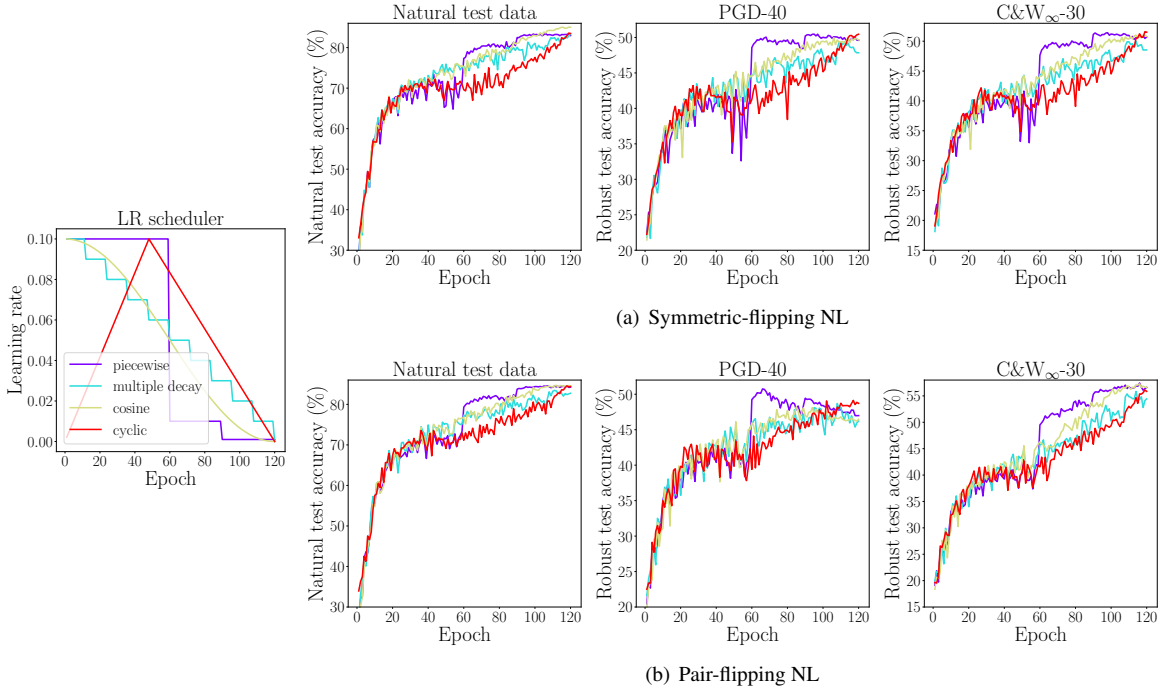


Figure 13: The leftmost panel shows the learning rate w.r.t. epoch under different LR schedulers. Figures 13(a) and 13(b) demonstrate the learning curves of AT-NoiLIn under various LR schedulers using symmetric-flipping NL and pair-flipping NL, respectively.

AT-NoiLIn uses the comparable training time with AT-LS. Both AT-NoiLIn and AT-LS using ResNet-18 on CIFAR-10 dataset spent about 256 seconds per training epoch evaluated on a GeForce RTX 2080 Ti GPU. It is owing to that the GPU can parallelly conduct the log operation for each data. That is, for each adversarial data \tilde{x} , the GPU only needs to conduct one log operation on all C elements of $p(\tilde{x})$ simultaneously.

But when AT-LS is conducted on the dataset which contains more classes (C is larger), such as ImageNet [12] dataset, the GPU may need to conduct at least more than one log operation for each data. Since the whole tensor of $p(\tilde{x})$ is too large for the limited GPU memory, $p(\tilde{x})$ has to be segmented into several small tensors that satisfying GPU memory for log operation. By contrast, AT-NoiLIn only needs to conduct one log operation on the \tilde{y} -th element of $p(\tilde{x})$ in this case. Therefore, NoiLIn framework is better than AT-LS from the perspective of computational efficiency.

F NoiLIn under Different Learning Rate Schedulers

We conducted AT-NoiLIn under different LR schedulers using ResNet-18 on CIFAR-10 dataset. All the training settings, such as the optimizer and hyperparameters of noise rate, kept exactly same as Section 5.1

Table 5: Evaluations of AT-NoiLIn using ResNet-18 on CIFAR-10 dataset under various LR schedulers. We reported the test accuracy of the best checkpoint and that of last checkpoint as well as the gap between them—“best/last (gap)”.

Defense	LR scheduler	Natural	C&W $_{\infty}$ -100	AA
Standard AT [20]	piecewise	81.97/84.76 (+2.79)	49.53/45.12 (-4.71)	48.09/43.30 (-4.79)
AT-NoiLIn (Symmetric)	piecewise	82.97/83.86 (+0.89)	51.21/50.36 (-0.85)	48.74/47.93 (-0.81)
	multiple decay	81.74/83.35 (+1.61)	49.42/48.59 (-0.83)	47.50/46.22 (-1.28)
	cosine	84.86/85.02 (+0.16)	50.83/50.59 (-0.24)	48.24/48.08 (-0.16)
	cyclic	83.48/83.48 (+0.00)	51.41/51.41 (+0.00)	49.05/49.05 (+0.00)
AT-NoiLIn (Pair)	piecewise	81.29/84.26 (+2.97)	51.35/ 56.27 (+4.92)	48.30/46.59 (-1.71)
	multiple decay	81.21/82.75 (+1.54)	50.87/54.01 (+3.14)	46.28/45.14 (-1.14)
	cosine	81.69/84.59 (+2.90)	53.09/56.06 (+2.97)	46.75/45.31 (-1.44)
	cyclic	84.34/84.34 (+0.00)	55.58/55.58 (+0.00)	47.75/ 47.75 (+0.00)

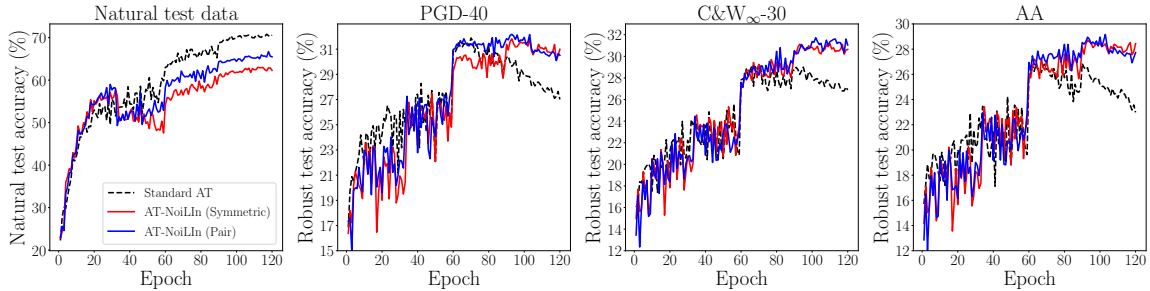


Figure 14: The learning curves of AT-NoiLIn under $\epsilon_{\text{train}} = 16/255$. Robust test accuracy was evaluated on adversarial test data bounded by $\epsilon_{\text{test}} = 16/255$.

except the LR scheduler. The learning rate w.r.t. epoch under different LR schedulers is shown in the leftmost panel of Figure 13. We demonstrated the learning curves of AT-NoiLIn (Symmetric) in Figure 13(a) and AT-NoiLIn (Pair) in Figure 13(b) under various LR schedulers. Figure 13 clearly indicates NoiLIn can mitigate robust overfitting under all different LR schedulers.

Further, we reported the test accuracy of the best checkpoint and that of the last checkpoint as well as the gap between them in Table 5. We observed the gap between test accuracy of the best checkpoint and that of the last checkpoint largely narrows with automatic NL injection, which again indicates NL injection can relieve overfitting. Moreover, Table 5 shows AT-NoiLIn under cyclic LR decay simply obtains the best checkpoint at the last epoch (the gap is exactly +0.00), which suggests AT-NoiLIn under cyclic LR scheduler can help save the time for selecting the best checkpoint. Note that for selecting the best checkpoint, it is time-consuming to gain the robust test accuracy based on AA attack for ResNet-18 and PGD-10 attack for Wide ResNet over all training epochs.

G NoiLIn under Larger ϵ_{train}

In this section, we compared standard AT and AT-NoiLIn under larger ϵ_{train} using ResNet-18 on CIFAR-10 dataset. The training settings of standard AT and AT-NoiLIn kept same as Section 5.1 except ϵ_{train} . We sampled ϵ_{train} from $\{8/255, 10/255, 12/255, 14/255, 16/255\}$. Robust test accuracy was evaluated on adversarial data bounded by L_{∞} perturbations with $\epsilon_{\text{test}} = \epsilon_{\text{train}}$. The step size α for PGD was $\epsilon/4$. In Figure 14 and Figure 15, on-the-fly NL was generated by symmetric-flipping (red color) and pair-flipping (blue color), respectively.

We demonstrated the learning curves of standard AT and AT-NoiLIn under $\epsilon_{\text{train}} = 16/255$ in Figure 14. We found both red and blue lines are above the black line in the right three panels of Figure 14. It suggests automatic NL injection largely relieves the serious issue of robust overfitting under larger ϵ_{train} and improves adversarial robustness evaluated under larger ϵ_{test} .

In Figure 15, we reported the test accuracy evaluated at the best checkpoint under different ϵ . Note that we

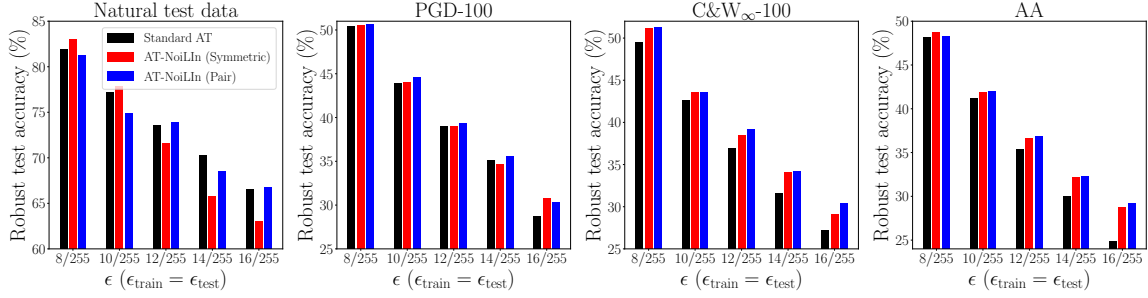
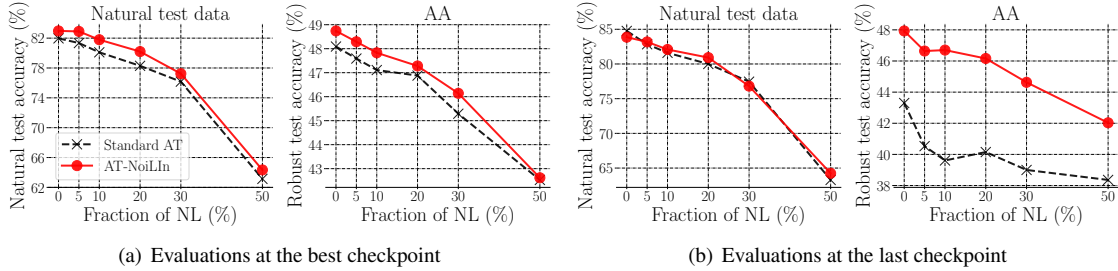


Figure 15: Comparisons between standard AT and AT-NoiLIn under larger ϵ_{train} . Note that ϵ_{test} for adversarial test data equaled to ϵ_{train} . We reported the test accuracy evaluated at the best checkpoint.



(a) Evaluations at the best checkpoint

(b) Evaluations at the last checkpoint

Figure 16: Comparisons between standard AT and AT-NoiLIn on noisy-label training set containing different fractions of NL.

set testing perturbation bound $\epsilon_{\text{test}} = \epsilon_{\text{train}}$ for the robust models trained under ϵ_{train} . The performance of AT-NoiLIn (both red and blue pillars) clearly exceeds that of standard AT (black pillars) due to automatic NL injection impeding robust overfitting.

H NoiLIn under Noisy-label Training Set

We conducted standard AT and AT-NoiLIn using symmetric-flipping NL on noisy-label training set which contains different fractions of NL using ResNet-18 on CIFAR-10 dataset. We randomly flipped a fraction of intact labels with uniform distribution from the original training set as the noisy-label version of training set. The fraction of NL was sampled from $\{0\%, 5\%, 10\%, 20\%, 30\%, 50\%\}$. Note that when the fraction of NL is 0%, the training set is exactly intact. The training settings of standard AT and AT-NoiLIn kept same as Section 5.1. We showed the performance of standard AT (black lines) and AT-NoiLIn (red lines) using symmetric-flipping NL on noisy-label training set containing different fractions of NL in Figure 16.

In Figure 16, as the fraction of NL increases, both standard test accuracy and robust test accuracy of standard AT and AT-NoiLIn decrease (both black and red lines drop). This phenomenon indicates intrinsic NL in noisy-label training set leads to vulnerability of generalization and robustness [28].

With automatic NL injection, we found both standard test accuracy and robust test accuracy achieve improvement at the best checkpoint since red lines are always above black lines in Figure 16(a). Moreover, we observed red line is always above black line in the right panel of Figure 16(b). It indicates automatic NL injection can alleviate the issue of robust overfitting consistently on noisy-label training set. Therefore, we propose to employ our NoiLIn framework even if the training set is intrinsically noisy-label.